

# Photoluminescence and Raman Scattering of Silicon Nanopowders

N. N. Ovsyuk<sup>a</sup>, V. A. Volodin<sup>b, c</sup>, and Prafulla K. Jha<sup>d</sup>

<sup>a</sup>Institute for Geology and Mineralogy, Siberian Branch, Russian Academy of Sciences, Novosibirsk, 630090 Russia

<sup>b</sup>Institute of Semiconductor Physics, Siberian Branch, Russian Academy of Sciences, Novosibirsk, 630090 Russia

<sup>c</sup>Novosibirsk State University, Novosibirsk, 630090 Russia

<sup>d</sup>Department of Physics, Maharaja Krishnakumarsinhji Bhavnagar University, Bhavnagar-364001, India

e-mail: ovsyuk@igm.nsc.ru

**Abstract**—Nanopowders obtained by evaporating silicon ingots with a powerful electron beam having an electron energy of 1.4 MeV in an Ar atmosphere are investigated. The nanopowders are studied by means of photoluminescence (PL) and Raman scattering (RS) spectroscopy. In simulating the PL spectra, the recombination energy dependences for the nanocrystals were found to be almost equal in vacuum and in silicon dioxide cores, allowing us to determine the average particle radius, which coincided with estimates obtained by analyzing the Raman spectra using an improved model of phonon localization that considers phonon dispersion in terms of quasi-momentum and direction.

DOI: 10.3103/S1062873813090335

## INTRODUCTION

The current interest in silicon nanopowders is due both to the fundamental scientific interest in silicon nanocrystals, and to the possibility of their practical application. In the last decade, scientists around the world have worked to develop new light-emitting diodes based on silicon nanocrystals. The reduction in particle size is known to generate uncertainty in the momentum of the charge carriers localized inside the particles. Direct transitions of electrons can thus occur as a consequence of electron-hole pair recombination, which is not observed in crystalline silicon (as indirect material), where recombination requires phonon participation. In addition, silicon nanocrystals are a promising material for memory cells, since they have such advantages as higher recording density and lower voltage in the recording process, compared to conventional cells. Nanocrystals of different sizes emit light with different wavelengths and can therefore be used as an alternative to conventional organic fluorescent dyes for labeling biomolecules [1, 2]. In contrast to conventional dyes, these materials are very photostable. In addition, a single source can excite several colors: the absorption spectra are actually quite wide, and the radiation is limited to a narrow band centered on the wavelength characteristic of nanocrystals of the given size.

In this work, we investigated nanopowders produced using the ELV-6 direct-action electron accelerator at the Budker Institute of Nuclear Physics, Siberian Branch, Russian Academy of Sciences. The accelerator was equipped with a system for emitting the beam into the atmosphere. The energy of bombarding electrons was 1.4 MeV. The power of the elec-

tron beam was high enough to evaporate a bulk silicon sample in an argon atmosphere at a gas pressure slightly higher than atmospheric. Silicon nanopowders were collected on a special filter and subsequently stored in the open atmosphere; they were thus coated with a silicon dioxide layer.

Figure 1 shows the PL spectrum of silicon nanopowder at room temperature. This spectrum presents a broad peak centered at a wavelength of 580 nm, corresponding to a recombination energy of 2.1 eV, while the forbidden band for silicon is 1.1 eV. This difference in 1 eV is due to quantum-size effects in the silicon nanocrystals. The broad peak width is likely associated with the size dispersion of the nanocrystals. To simulate the PL spectra of the silicon nanocrystals, the quantum-mechanical problem of calculating the

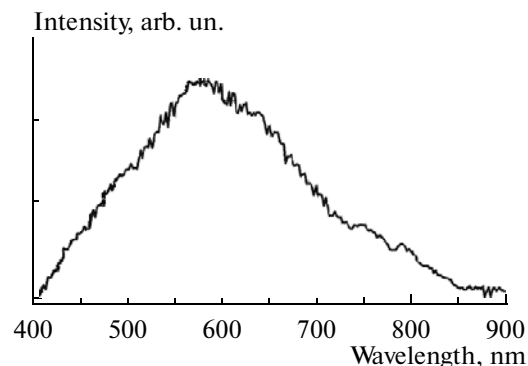


**Fig. 1.** Photoluminescence spectrum of Si nanopowder. An  $N_2$  pulse laser ( $\lambda = 337$  nm) was used for excitation,  $T = 300$  K.

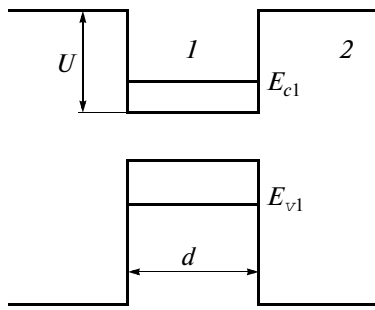


Fig. 2. Band structure of Si nanocrystal in a dielectric matrix.

energy levels in a quantum well was solved for a spherically symmetric case. In the model of effective masses, only the continuity of wave functions derivatives near the boundary between a spherical well and barrier is traditionally assumed. Such boundary conditions are correct when the effective mass is constant. In our case, there is a discontinuity in the effective mass at the boundary of quantum dot that strongly influences the position of the energy levels of electrons and holes. We therefore use the condition of flow continuity, which at the mass depending on the coordinate

is reduced to the relation  $\frac{\Psi_1'}{m_1} = \frac{\Psi_2'}{m_2}$ , where  $m_1$  and  $m_2$

are the effective masses of carriers in the first and second regions, respectively [3]. The equality of wave functions at the boundary remains valid, and the values of wave functions at the boundary of regions 1 and 2 are equal; i.e.,  $\psi_1 = \psi_2$ . Since the particles are in contact with air and have many free bonds, they should be covered by oxide layer. It is therefore logical to calculate the energy levels of the Si–SiO<sub>2</sub> heterostructure. The band diagram for a nanocrystal located inside the dielectric is presented in Fig. 2. But to begin, let us calculate the energy of a simpler nanocrystal system in a vacuum when barriers differ for electrons and holes, and the width of the optical gap can also change greatly. For the electrons in the conduction band, the value of the exit barrier in a vacuum is determined by the electron affinity, while for electrons in the valence band it depends on the energy of the photoemission threshold. The problem of finding the energy levels of electrons and holes in a symmetrical sphere was solved by Landau in [4]. In spherical coordinates, the Schrödinger equation can be written as

$$-\frac{\hbar^2}{2m} \left[ \frac{1}{r^2} \frac{\partial}{\partial r} \left( r^2 \frac{\partial}{\partial r} \right) + \frac{1}{r^2 \sin \theta} \frac{\partial}{\partial \theta} \left( \sin \theta \frac{\partial}{\partial \theta} \right) + \frac{1}{r^2 \sin^2 \theta} \frac{\partial^2}{\partial \varphi^2} \right] \psi(\vec{r}) + U(r) \psi(\vec{r}) = E \psi(\vec{r}).$$

We separate the variables and seek the wave function in the form of the product of two functions:  $\psi(\vec{r}) = R(r) \times Y(\theta, \varphi)$ , one of which depends only on  $r$ , while the other depends on the  $\theta$  and  $\varphi$  angles.

For the radial dependence of wave function for the case when  $R(r) = \frac{\chi(r)}{r}$ , we then obtain the equation

$$-\frac{\hbar^2}{2m} \frac{\partial^2 \chi(r)}{\partial r^2} + \left[ U(r) + \frac{l(l+1)\hbar^2}{2mr^2} \right] \chi(r) = E \chi(r). \quad (1)$$

where  $l$  is the orbital angular momentum. Inside the well, potential  $U$  is a negative constant; outside the quantum dot, the value of the potential is zero. Thus,  $U$  is the value of barrier. Even for zero orbital angular momentum, this problem can be solved analytically only for infinite barriers, when the wave function outside the quantum dot is zero and inside the quantum dot  $\chi(r) = A \cdot \sin(kr)$ . Since energy  $E$  is measured from the bottom of the well, parameter  $k$  depends on  $E$  as

$k = \left[ \frac{2mE}{\hbar^2} \right]^{1/2}$ , and we can find the value of energy  $E$

from the boundary condition. The wave function at the interface should be zero. If the radius of the quantum dot is  $a$  ( $a = d/2$ , where  $d$  is the diameter of a nanocrystal) (Fig. 2), from the boundary conditions  $k_0 a = n\pi$ , where  $n$  is integer. Therefore,

$$E_n = \frac{\hbar^2}{2m} \left( \frac{\pi n}{a} \right)^2. \quad (2)$$

With finite barriers, the wave function does not vanish at the dot–barrier interface. The electrons can tunnel into barriers. We must therefore solve Eq. (1) numerically with the boundary conditions for the wave function and its derivative [3]. If  $l = 0$ , the Schrödinger equation in the first region (inside the nanocrystal) can be written as

$$-\frac{\hbar^2}{2m_1} \chi_1''(r) = \frac{\hbar^2 k^2}{2m_1} \chi_1(r), \quad (3)$$

where  $\chi(r) = rR(r)$ ,  $R(r)$  is the radial part of the wave function if we separate the variables in spherical coordinates. The general solution to this equation is  $\chi(r) = A \sin(kr) + B \cos(kr)$ , however,  $\chi(0) = 0$ , so  $\chi_1(r) = A \sin kr$ . In the second area (outside the nanocrystal), the Schrödinger equation is

$$-\frac{\hbar^2}{2m_2} \chi_2''(r) + U \chi_2 = \frac{\hbar^2 k^2}{2m_2} \chi_2(r), \quad (4)$$

so  $\chi_2(r) = B \exp(\xi r) + C \exp(-\xi r)$ , where  $\xi = \sqrt{\frac{2m_2 U}{\hbar^2} - k^2}$ . Combining the solutions at the interface (where  $r = a$ ) and considering that according to the

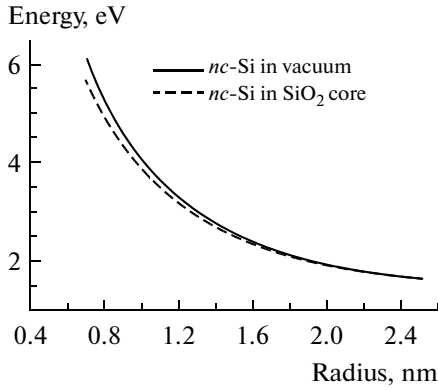


**Fig. 3.** Comparison of the recombination energy's dependence on particle radius for the *nc*-Si–vacuum and *nc*-Si–SiO<sub>2</sub> systems.

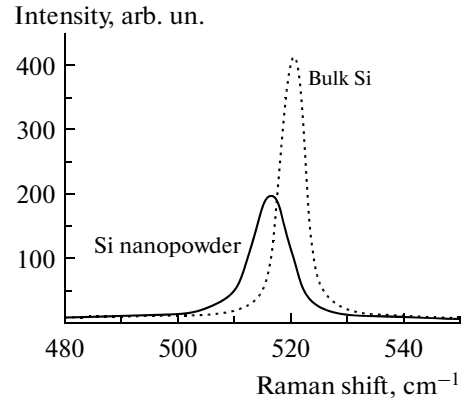


**Fig. 4.** Raman spectra of bulk Si (dashed line) and Si nanopowder produced by electron beam evaporation in an argon atmosphere.

normalization of wave function  $B = 0$  (the function cannot grow at infinity), we find

$$\frac{m_2}{m_1} [ka \cos(ka) - \sin(ka)] + \left[ 1 + \sqrt{\frac{2m_2 U a^2}{\hbar^2} - (ka)^2} \right] \sin(ka) = 0. \quad (5)$$

This equation was solved numerically, and discrete values of wave vector  $\vec{k}_0$  (depending on the radius of quantum dot  $a$ ) were found. The values of the energy levels were then found:  $E = \frac{\hbar^2 k_0^2}{2m_1}$ , since the value of  $\vec{k}_0$

depends on the radius of quantum dot  $a$ . The dependence of the energy levels on quantum dot (particle) radius was therefore determined. In crystalline silicon, the effective electron mass is known to be anisotropic. There are longitudinal and transversal masses  $m_{\parallel} = 0.98m_0$  and  $m_{\perp} = 0.2m_0$ , where  $m_0$  is the free electron mass. Since the orientation of nanocrystals is arbitrary, we must use the average effective electron mass in silicon. The energy of an electron in a nanocrystal is  $E = \frac{\hbar^2 k_x^2}{2m_x} + \frac{\hbar^2 k_y^2}{2m_y} + \frac{\hbar^2 k_z^2}{2m_z}$ , where  $m_x = m_y = m_{\perp}$ ,  $m_z = m_{\parallel}$ .

Since  $E = \frac{\hbar^2 k^2}{2m_{\text{ef}}}$ , we can obtain the effective mass:  $m_{\text{ef}} = 3m_{\perp} \times m_{\parallel} / (2m_{\perp} + m_{\parallel}) = 0.26m_0$ . The effective mass of the heavy holes in silicon is  $0.5m_0$ . The energy levels of light holes are lower, and can be excluded from consideration. This problem was solved for both the conduction and the valence band. In the case of silicon nanocrystals with a free interface,  $U = 4.05$  eV (the value of electron affinity of silicon). To calculate the energy level in the valence band, we must solve the self-consistent problem in which the barrier depends

on the level of energy. Since the energy level in the valence band is quite low ( $<1$  eV) relative to  $E_g + \chi = 5.15$  eV, we may assume that the value of the barrier  $U = 5.15$  eV. The recombination energy is obviously the sum of the energy levels and the band gap. We then calculate the energy levels for the Si–SiO<sub>2</sub> heterostructure: the band gap of silicon dioxide is 8.7 eV, while the electronic barrier is 3.2 eV for the Si–SiO<sub>2</sub> heterostructure and 4.3 eV for holes. The electron and hole effective masses in SiO<sub>2</sub> are  $m_e = 0.42m_0$  and  $m_h = 0.32m_0$ , respectively. Figure 3 compares the recombination energy dependence on the nanocrystal radius for the *nc*-Si–vacuum and *nc*-Si–SiO<sub>2</sub> systems. We can see that the dependence of the recombination energy of nanocrystals in a vacuum and in silica are close, which was not obvious for the difference between the barrier values for electrons and holes. We can see from Figs. 1 and 3 that the average nanocrystal radius is about 1.8 nm. The Raman spectrum in Fig. 4, in which a shift of the nanocrystal peak in the range of lower frequencies from the position of the bulk silicon Raman peak is observed, was also used to estimate the average size of the silicon nanocrystals. The shift and broadening of the optical phonon Raman peaks was a result of the law of phonon quasi-momentum conservation being suspended due to phonon confinement in nanocrystals [5, 6]. The law of quasi-momentum conservation was suspended in observance of the Heisenberg Uncertainty Principle.

It was assumed above that nanocrystals are spheres with diameter  $d$ . Assuming that at the boundary of a nanocrystal ( $a = L = d/2$ ) the phonon amplitude is  $1/e$  (the phonon amplitude at center of nanocrystal is unit), we can use the approach developed in [5, 6].

For crystals with diamond-type lattices [8], there are generally six phonon branches with dispersions

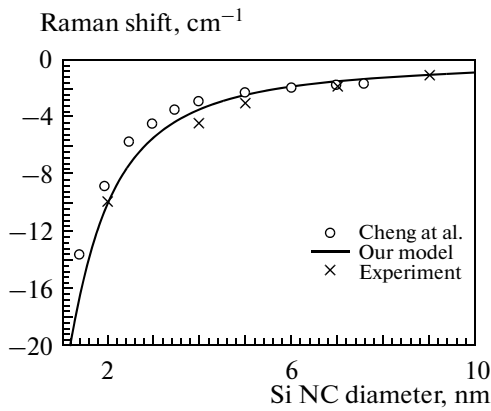


**Fig. 5.** Shift in the position of the Raman peak for optical phonons confined in Si NCs of various sizes, relative to the position of the Raman peak for bulk Si. The circles correspond to the data calculated by Ren and Cheng [7]; the solid curve corresponds to our results, obtained using our improved model (dispersion was calculated in the Keating model with allowance for the angular phonon dispersion). Crosses represent our experimental data.

$\omega_i(q)$ , so the first order Raman spectrum for phonon weighting function  $W(r, L) = \exp(-4r^2/L^2)$  is:

$$I(\omega) = A \sum_{i=1}^6 \int_0^1 [n(\omega_i(q)) + 1] \times \frac{4\pi q^2 \exp(-q^2 r_0^2/4)}{(\omega - \omega_i(q))^2 + (\Gamma/2)^2} dq, \quad (6)$$

where  $n(\omega)$  is the Bose–Einstein factor,  $\omega_i(q)$  is phonon dispersion of a phonon band, and  $\Gamma$  is the full width at the half maximum of the Raman peak of a single phonon,  $r_0$  is radius of NCs.

Wave numbers were varied from 0 up to  $q_{\max}$  (the edge of the Brillouin zone). For directions with high symmetry ( $\langle 100 \rangle$  and  $\langle 111 \rangle$ ) it should be noted that some phonon branches are degenerated. The density of states for phonons was proportional to  $q^2 dq$ .

Our model was considerably improved by considering the dispersion of phonons not only in the magnitude of quasi-momentum [5–7], but also in its direction [8]. Considerable refinement of the model was achieved by using the familiar Keating model [9] to calculate phonon dispersion instead of approximating it by

empirical expressions, as was done in earlier approaches. Calculations based on this model allow us to determine the sizes of germanium nanocrystals more precisely by analyzing the Raman spectra. Figure 5 shows the difference between the positions of the Raman peaks of nanocrystals and single-crystal silicon, showing that the results of our model calculations are in better agreement with the experimental data and the estimates obtained from our analysis of the PL spectra.

## CONCLUSIONS

Our study of silicon nanopowder produced by evaporating bulk silicon with a powerful electron beam suggests that such nanopowders contain nanocrystals with average sizes of  $\sim 3$ – $4$  nm. These powders generate a photoluminescence signal in the visible region of the spectrum and thus provide opportunities for developing light-emitting structures based on them.

## ACKNOWLEDGMENTS

This work was supported by the Federal Target Program “Research and Scientific–Pedagogical Personnel of Innovative Russia” for 2009–2013, project no. 14.B37.21.1069.

## REFERENCES

1. Han, M., Gao, X., Su, J.Z., and Nie, S., *Nat. Biotechnol.*, 2001, vol. 19, p. 631.
2. Rosenthal, S.J., *Nat. Biotechnol.*, 2001, vol. 19, p. 621.
3. Bastard, G., *Phys. Rev. B*, 1981, vol. 24, p. 5693.
4. Landau, L.D. and Lifshits, E.M., *Kvantovaya mekhanika. Nerelyativistskaya teoriya* (Quantum Mechanics: Non-Relativistic Theory) Moscow: Nauka, 1989, p. 767.
5. Campbell, I.H. and Fauchet, P.M., *Solid State Commun.*, 1986, vol. 58, p. 739.
6. Paillard, V., Puech, P., Laguna, M.A., and Carles, R., *J. Appl. Phys.*, 1999, vol. 86, p. 1921.
7. Cheng, W. and Ren, S.-F., *Phys. Rev. B*, 2002, vol. 65, p. 205305.
8. Volodin, V.A. and Sachkov, V.A., *JETP*, 2013, vol. 116, no. 1, p. 87.
9. Keating, P.N., *Phys. Rev.*, 1966, vol. 145, p. 637.

*Translated by E. Kapinus*